

Communication

# Anti-Amyloid Aggregation Activity of Black Sesame Pigment: Toward a Novel Alzheimer's Disease Preventive Agent

Lucia Panzella <sup>1,\*</sup> , Thomas Eidenberger <sup>2</sup> and Alessandra Napolitano <sup>1</sup> 

<sup>1</sup> Department of Chemical Sciences, University of Naples "Federico II", Via Cintia 4, I-80126 Naples, Italy; alesnapo@unina.it

<sup>2</sup> School of Engineering and Environmental Sciences, Upper Austria University of Applied Sciences, Stelzhamerstraße 23, 4600 Wels, Austria; Thomas.Eidenberger@fh-wels.at

\* Correspondence: panzella@unina.it; Tel.: +39-081-674131

Received: 22 February 2018; Accepted: 15 March 2018; Published: 16 March 2018

**Abstract:** Black sesame pigment (BSP) represents a low cost, easily accessible material of plant origin exhibiting marked antioxidant and heavy metal-binding properties with potential as a food supplement. We report herein the inhibitory properties of the potentially bioaccessible fraction of BSP following simulated gastrointestinal digestion against key enzymes involved in Alzheimer's disease (AD). HPLC analysis indicated that BSP is transformed under the pH conditions mimicking the intestinal environment and the most abundant of the released compounds was identified as vanillic acid. More than 80% inhibition of acetylcholinesterase-induced aggregation of the  $\beta$ -amyloid A $\beta$ 1-40 was observed in the presence of the potentially bioaccessible fraction of BSP, which also efficiently inhibited self-induced A $\beta$ 1-42 aggregation and  $\beta$ -secretase (BACE-1) activity, even at high dilution. These properties open new perspectives toward the use of BSP as an ingredient of functional food or as a food supplement for the prevention of AD.

**Keywords:** black sesame; Alzheimer's disease; vanillic acid; simulated digestion; acetylcholinesterase; butyrylcholinesterase;  $\beta$ -amyloid;  $\beta$ -secretase

## 1. Introduction

Alzheimer's disease (AD) is a neurodegenerative disorder that represents the most common type of dementia among elderly people. Thus far, low levels of acetylcholine (ACh), oxidative stress, disequilibrium of metals metabolism, and  $\beta$ -amyloid (A $\beta$ ) deposits have been considered to play definite roles in AD pathogenesis [1–5]. There is in particular a general consensus that A $\beta$  is the main culprit of a straightforward cascade process that begins with its increased formation by processing of the amyloid precursor protein (APP) by  $\beta$ -secretase (BACE-1) and acetylcholinesterase (AChE)-induced or self-aggregation into oligomers and fibrils [6,7]. Synaptic dysfunction, tau protein hyperphosphorylation and aggregation, neuroinflammation, and oxidative stress would then follow, leading eventually to neuronal death and neurotransmitter deficits [8,9]. The first and so far sole marketed anti-Alzheimer drugs are the AChE inhibitors donepezil, rivastigmine, and galantamine, which increase the ACh levels [10]; these drugs, however, are effective only for symptomatic treatment of AD, since they are not able to prevent the progression of the disease. Other drugs, such as memantine, have proved to be effective in the treatment of both mild and moderate-to-severe AD by reducing excitotoxicity [11]. In the past years, there has been intense research activity for developing drugs able to inhibit A $\beta$  formation or aggregation [12]. However, a number of clinically advanced A $\beta$ -directed drug candidates have recently failed to show efficacy over placebo. This has been ascribed, at least in part, to the fact that AD might not result from a single process but from a robust network of

interconnected events, whereby A $\beta$  aggregation is just one of the causes. Therefore, therapies with combination of drugs [13] or the development of multitarget anti-Alzheimer drugs [14] has become a primary objective. These have been usually designed to hit at least A $\beta$  formation and aggregation and AChE activity, especially prompted by the finding that AChE can bind A $\beta$  and accelerate its aggregation through the so-called peripheral anionic site (PAS) [15,16]. The design of inhibitors able to simultaneously reach both the PAS and the catalytic anionic site (CAS) of AChE has therefore emerged as a promising source of multitarget anti-Alzheimer compounds [17–21].

Phenolic compounds have been the focus of increasing interest over the past decades because of a range of biological properties that have been implicated to account for the lower risk of malignant neoplasms and of cardiovascular and neurodegenerative diseases such as AD [22–26], although safety issues in the production of food supplements should not be disregarded [27,28]. In particular, sesame lignans, such as sesaminol and sesamol, have been shown to efficiently inhibit AChE and A $\beta$  oligomerization and fibril formation [29–32]. Little attention has been directed so far to the potential AD prevention properties of the insoluble pigment of black sesame seeds. Black sesame (*Sesamum indicum* L.) seeds, traditionally used in Chinese folk medicine and as food for humans in China and other East Asian countries, have attracted interest because of their potent antioxidant activity, superior to that of white sesame seeds [33–35]. This activity has been commonly attributed to a number of soluble lipids of the lignan type, including primarily sesamin and sesamol [36] but also sesaminol, sesamol, and pinoresinol [37,38], which occur in sesame seeds partly as glycosylated derivatives [39] and have been shown to display several health beneficial effects [40–44]. More recently, several studies have been focused on the peculiar properties of the insoluble pigment of black sesame seeds [45]. In particular, we recently developed an improved purification procedure to obtain black sesame pigment (BSP), involving fat removal by treatment of ground black sesame seeds with dichloromethane followed by an optimized hydrolytic protocol with 6 M HCl, at 100 °C, overnight [46]. The black pigment thus obtained displayed good antioxidant efficiency in the 2,2-diphenyl-1-picrylhydrazyl (DPPH) radical assay, good ferric ion-reducing capacity and potent antinitrosating properties. BSP was also shown to efficiently bind heavy metals like lead, cadmium, and mercury [47] that are commonly found in food and are known to cause impairment of the immune and central nervous systems [48,49].

The importance of evaluating the actual bioavailability of phytochemicals in food based on data concerning their absorption, metabolism, tissue and organ distribution, and excretion has been increasingly appreciated [50–52]. Such studies carried out on animals or human subjects are necessarily complex, expensive, and lengthy. This is the reason why different *in vitro* procedures that mimic the physiochemical and biochemical conditions encountered in the gastrointestinal tract have been developed, providing preliminary data on the potential bioavailability of different components of the food under evaluation [53–57].

We report herein the results of chemical assays to evaluate the potential AD preventive effect of the bioavailable fraction of BSP following a simulated gastrointestinal digestion. The method consisted of two sequential steps, that is an initial pepsin/HCl digestion, at pH 1.7, for 2 h at 37 °C, followed by a digestion with bile salts/pancreatin for 2 h at 37 °C at pH 7.5, to simulate pH and transit times in the stomach and small intestine, respectively.

## 2. Results and Discussion

### 2.1. Structural Investigation of BSP Phenolic Components

Based on the previous finding that vanillic acid (VA) represents one of the main fragments following chemical degradation of BSP [46] and on the results of total reflectance Fourier transform infrared (ATR-FTIR) and solid-phase NMR experiments [47], it has been proposed that *ortho*-methoxyhydroxy units are represented to a significant extent in the backbone of BSP, although *ortho*-diphenols and phenolic acids are present as well. To further confirm this hypothesis, BSP was subjected to alkali fusion under reducing conditions. HPLC/DAD/MS analysis of the ethyl acetate

extractable fraction indicated the presence of five main products, three of which were identified by comparison with authentic reference standards as 3,4-dihydroxybenzoic acid, 4-hydroxybenzoic acid and VA (Figure 1, Figures S1 and S2). These results confirm the presence of phenol, *ortho*-diphenol, and *ortho*-methoxyphenol moieties in BSP.

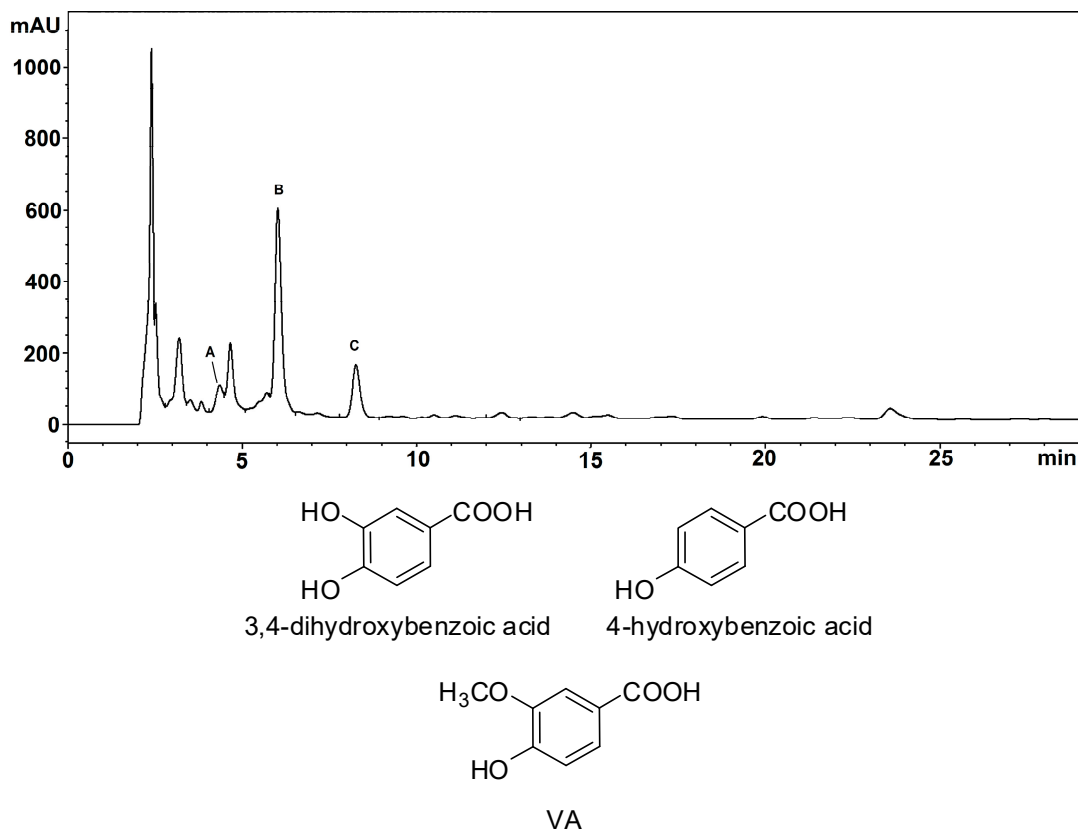


**Figure 1.** HPLC trace (detection at 254 nm) of the ethyl acetate extractable fraction of the alkali fusion mixture of BSP. Peak A: 3,4-dihydroxybenzoic acid; peak B: 4-hydroxybenzoic acid; peak C: VA. The chromatographic separation was performed on an octadecylsilane (ODS) column (325 × 4.60 mm, 5 μm), at a flow rate of 0.9 mL/min. The mobile phase was a 0.02 M ammonium acetate buffer, pH = 3.5 (solvent A)/methanol (solvent B) gradient as follows: from 5% to 25% B, 0–20 min. Chemical structures of the identified compounds are also shown.

## 2.2. Simulated Gastrointestinal Digestion of BSP

Among the different protocols reported in the recent literature mimicking the physiochemical and biochemical conditions encountered in the gastrointestinal tract, a procedure was chosen that had been used to investigate release of phenolic compounds from food matrix [58,59]. A suspension of the pigment at 5 mg/mL was subjected to two sequential steps: an initial pepsin/HCl digestion for 2 h at 37 °C to simulate gastric conditions, followed by a digestion with bile salts/pancreatin for 2 h at 37 °C at pH 7.5 to simulate small intestine conditions. An oral digestion step using α-amylase was not included in the digestion protocol as the acid treatment used to obtain BSP likely produces efficient removal of the carbohydrate components [47]. In order to assess the potential serum availability of the components released from the pigment after complete digestion, a model was used consisting of a cellulose dialysis tube (molecular mass cutoff 12 KDa), containing sufficient sodium bicarbonate to neutralize the acidity of the mixture after the initial pepsin digestion, immersed into the mixture containing the pigment at the time the bile salts/pancreatin digestion treatment starts. The bicarbonate is slowly released into the mixture and some of the components are allowed to enter the tube. After 2 h

at 37 °C the solution outside the dialysis tubing was taken as the OUT sample, representing the material remaining in the gastrointestinal tract, and the solution that entered the dialysis tubing was taken as the IN sample representing the material entering the serum. Care should be taken, however, in extrapolating the results to the *in vivo* situation because the partition of phenols into the dialysis tubing is dependent also on their diffusion rates and stability. HPLC analysis of the IN sample (Figure 2, green trace) indicated a complex pattern of products, some of which were observed also in a control mixture not containing BSP and therefore clearly due to enzyme/bile salts-derived products (Figure 2, red trace). The remaining components were also present in the mixture of the pigment exposed to the pH conditions of the simulated digestion treatment but without added enzymes and bile salts (Figure 2, purple trace), indicating that BSP is able to release low molecular weight compounds under the conditions of the intestinal transit without the need of enzyme action. Of these compounds, only that eluted at 12.5 min was quantitatively extracted in ethyl acetate (Figure 2, blue trace). No appreciable release of any of these compounds could be observed at the acidic pH simulating gastric conditions (not shown).

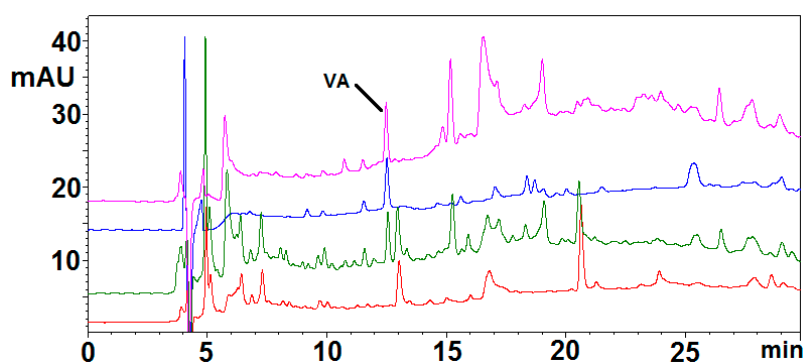


**Figure 2.** HPLC traces of the IN samples obtained from simulated gastrointestinal digestion of BSP. Green: IN sample from BSP digestion. Blue: ethyl acetate extractable fraction of the IN sample. Red: IN sample from a control mixture containing only enzyme and bile salts (without BSP). Purple: IN sample from BSP digestion without enzyme and bile salts. The chromatographic separation was performed on a ODS column (250 × 4.60 mm, 5 μm), at a flow rate of 0.7 mL/min. The mobile phase was a 1% formic acid (solvent A)/methanol (solvent B) gradient as follows: from 5% to 90% B, 0–45 min.

LC/ESI+/MS analysis allowed to identify the product eluted at 12.5 min as VA (pseudomolecular ion  $[M + H]^+$  at  $m/z$  169), confirmed also by comparison of the chromatographic behavior with that of an authentic reference standard (Figure S3). This result is of considerable interest in the light of the several health beneficial properties of VA [60–64], first of all its neuroprotective activity [65,66]. The concentration of VA released in the IN sample was estimated to be as high as 6 μM. However, it should be considered that liver metabolism and the blood-brain barrier could potentially restrict the concentration of VA available in brain.

### 2.3. Determination of the Activity of BSP toward AD Drug Targets

The activity of the IN sample and, for comparison, of VA toward AD drug targets was evaluated by a number of validated chemical assays. Based on the results described above, to avoid interference by digestive enzymes and bile salts, the IN sample from BSP that has only been subjected to variations of pH was tested.

#### 2.3.1. AChE and BChE Inhibition Assay

The cholinergic hypothesis for AD suggests that cognitive deterioration is mainly caused by low levels of acetylcholine (ACh) because maintaining high ACh levels (via AChE inhibitors) has been

shown to alleviate these symptoms [67]. The AChE inhibition properties of VA were evaluated by the Ellman's method, using AChE from electricus eel and acetylthiocholine iodide as substrate, as described in several papers [68–70]. Indeed, it was not possible to test the IN sample since it exhibited a significant absorption at the detection wavelength used in the Ellman's method (412 nm) even at high dilution, therefore leading to interference. The percentage of inhibition as a function of log-scale concentration of VA is reported in Figure S4. More than 45% inhibition was observed with 180  $\mu\text{M}$  VA, whereas a ca. 15% inhibition was observed at 6  $\mu\text{M}$ , that is at the concentration released from BSP upon simulated gastrointestinal digestion.

BChE is another target of interest in the search for anti-Alzheimer drugs as this enzyme plays a critical role for ACh hydrolysis in the late stage of AD, when level of AChE in brain declines to 55–67% of normal values while BuChE increases to 120% of normal levels [71,72]. The inhibition activity of VA was evaluated as described above for AChE, using equine serum BChE and butyrylthiocholine iodide as the substrate. As shown in Figure S5, a maximum 27% inhibition was observed with 18  $\mu\text{M}$  VA, but a comparable inhibition (18%) as that determined in the AChE inhibition assay was observed at the potentially physiological concentration of 6  $\mu\text{M}$ .

### 2.3.2. AChE-Induced A $\beta$ 1-40 Aggregation Inhibition Assay

The inhibition properties of VA and the IN sample against AChE-induced amyloid aggregation were evaluated using the thioflavin T-based fluorescent method [69] and the amyloid A $\beta$ 1-40, which represent one of the main isoforms of A $\beta$  peptides [73,74]. A  $83 \pm 5\%$  inhibition was observed with 5  $\mu\text{M}$  VA, and a comparable value ( $83 \pm 7\%$ ) was obtained with a 20-fold diluted IN sample. These results are very encouraging in the light of the low, potentially physiological, concentrations tested, especially for the IN sample. Based on the concentration determined by HPLC analysis for VA in the IN sample (ca. 6  $\mu\text{M}$ ), these results would suggest that other components significantly contribute to the aggregation inhibition activity. The characterization of these compounds is currently underway.

Notably, the inhibition induced by BSP-related samples was higher than that reported for donepezil in a human erythrocytes AChE-induced A $\beta$ 1-40 aggregation assay ( $25.0 \pm 0.6\%$  at 100  $\mu\text{M}$ ) [75].

Compared with the results of the AChE inhibition assay (only 15% inhibition at 5  $\mu\text{M}$ ), these results would indicate a higher affinity of VA for PAS than for CAS of AChE.

### 2.3.3. $\beta$ -Amyloid Self-Aggregation Inhibition

The inhibitory activity of the samples against the spontaneous aggregation of amyloid A $\beta$ 1-42, which shows a significant increase with certain forms of AD [74,76], was determined using the thioflavin T based fluorometric assay as before. In this case a ca. 50% inhibition was observed with 6  $\mu\text{M}$  VA, reaching a ca. 90% value at 50  $\mu\text{M}$ . An even higher inhibition was observed with the IN sample (Figure 3). Under the same conditions, it was reported that 25  $\mu\text{M}$  donepezil did not show any inhibitory activity, whereas curcumin at 25  $\mu\text{M}$  showed 43% inhibition [75].

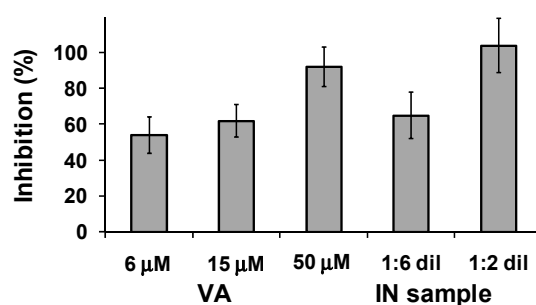


**Figure 3.** Inhibition of self-induced A $\beta$ 1-42 aggregation by VA and IN sample at different dilutions. Reported are the mean  $\pm$  SD values from at least three experiments.

Copper-induced  $\beta$ -amyloid aggregation has also been implicated in the etiology of AD [77]. The ability to inhibit copper-induced amyloid aggregation is related to the capacity of a compound to form copper chelates in order to retrieve the metal ion from the amyloid. This is not the case of VA, which did not form complexes with copper ions [78], so the possibility that VA could interfere with the copper-induced amyloid aggregation was not investigated because it is rather unlikely.

#### 2.3.4. BACE-1 Inhibition

BACE-1 catalyzes the first and rate-limiting step of the biosynthesis of  $\beta$ -amyloid peptide from APP, thereby constituting a primary target in the search for anti-AD drugs [79,80]. The BACE-1 inhibition assay was performed by employing a model peptide mimicking the APP sequence as substrate and the fluorescence resonance energy transfer (FRET) method [81]. An inhibition higher than 60% was caused by 60  $\mu$ M VA, but essentially no effect was observed at the potentially physiological concentration of 6  $\mu$ M. On the other hand, significant inhibition properties (15–33%) were found for the IN sample even at the high dilution used to eliminate any interference in the fluorescence measurement (Figure 4). As an example, previously reported  $IC_{50}$  values for known inhibitors of BACE-1 used as positive controls in BACE-1 FRET assay kits were ca. 12  $\mu$ M for morin [81], 7.4  $\mu$ M for quercetin [82], and 33 nM for the peptidomimetic inhibitor OM99-2 [83].

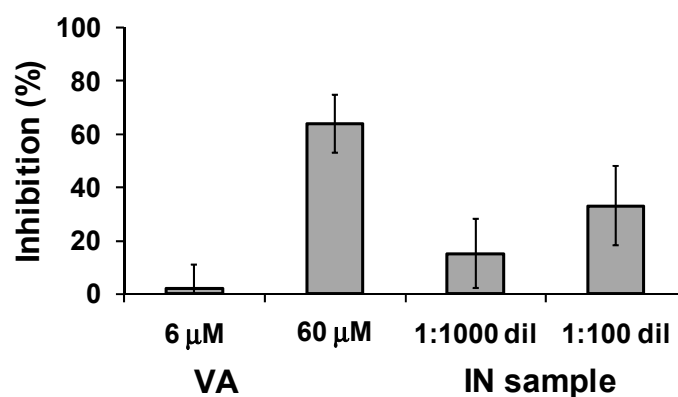


**Figure 4.** Inhibition of BACE-1 by VA and IN sample. Reported are the mean  $\pm$  SD values from at least three experiments.

### 3. Materials and Methods

#### 3.1. Materials

BSP was prepared from black sesame seeds (*Sesamum indicum* L.) as previously described [46]. Pepsin from porcine gastric mucosa, pancreatin from porcine pancreas, porcine bile extract, 4-hydroxy-3-methoxybenzoic acid (VA), 4-hydroxybenzoic acid, 3,4-dihydroxybenzoic acid, KOH, NaOH,  $Na_2S_2O_4$ , AChE from *Electrophorus electricus* (E.C.3.1.1.7, Type VI-S), acetylthiocholine iodide, 5,5'-dithiobis-2-nitrobenzoic acid (DTNB), BChE from equine serum (E.C.3.1.1.8), butyrylthiocholine iodide, thioflavin T, 1,1,1,3,3,3-hexafluoro-2-propanole (HFIP) and BACE1 activity detection kit were purchased from Sigma-Aldrich (Milan, Italy); synthetic  $A\beta$  1-40 and 1-42 (human sequence) were from Bachem (Bubendorf, Switzerland).

#### 3.2. General Experimental Methods

HPLC analysis of the alkali fusion mixtures was performed with an instrument equipped with a diode array detector (DAD). The chromatographic separation was performed on an octadecylsilane (ODS) column (325  $\times$  4.60 mm, 5  $\mu$ m), at a flow rate of 0.9 mL/min. The mobile phase was a 0.02 M ammonium acetate buffer, pH = 3.5 (solvent A)/methanol (solvent B) gradient as follows: from 5% to

25% B, 0–20 min. The principle detection wavelength was 254 nm. UV-VIS spectra were collected for all peaks in the range 200–600 nm. LC-MS analysis was performed with a system equipped with a quadrupole mass spectrometer with ESI source operating in negative ionization mode in the following conditions: nebulizer pressure 50 psi; drying gas (nitrogen) 11 L/min, 300 °C; capillary voltage 4500 V; fragmentor voltage 150 V. The chromatographic separation was performed as described above for HPLC analysis.

HPLC analysis of the simulated gastrointestinal digestion mixtures was performed with an instrument equipped with a UV-vis detector. The chromatographic separation was performed on a ODS column (250 × 4.60 mm, 5 µm), at a flow rate of 0.7 mL/min. The mobile phase was a 1% formic acid (solvent A)/methanol (solvent B) gradient as follows: from 5 to 90% B, 0–45 min. The detection wavelength was 254 nm. LC-MS analysis was performed with a system equipped with a UV-vis detector and a quadrupole mass spectrometer with ESI source operating in positive ionization mode in the following conditions: nebulizer pressure 50 psi; drying gas (nitrogen) 10 L/min, 350 °C; capillary voltage 4000 V; fragmentor voltage 50 V. The chromatographic separation was performed as described above for HPLC analysis.

### 3.3. Alkali Fusion of BSP

Solid and finely grinded KOH, NaOH, and Na<sub>2</sub>S<sub>2</sub>O<sub>4</sub> were mixed in a 1:1:0.02 ratio (i.e., 100 mg/100 mg/2 mg) in a pyrex tube and kept at 240 °C for 3 min (until fusion of the reagents). 20 mg of BSP were then added and the mixture was kept at 240 °C for 10 min. After cooling to room temperature, 10 mL of a 1% sodium dithionite solution were added. After addition of 0.7 mL of acetic acid, the mixture was extracted with ethyl acetate (3 × 15 mL) and the combined organic layers were dried over sodium sulfate and evaporated to dryness. The solid residue was reconstituted in mobile phase, cleared by filtration (0.2 µm syringe filters), and analyzed by HPLC/DAD/MS.

### 3.4. Simulated Gastrointestinal Digestion of BSP

The procedure was adapted from a reported method [58,59]. BSP (100 mg) was finely suspended by use of a glass/glass Tenbroeck grinder in 2.5 mL of distilled water. The suspension was made up to 20 mL with distilled water (final concentration of BSP 5 mg/mL) and adjusted to pH 1.7 with 5 M HCl. 315 Units/mL pepsin were added and the mixture was incubated at 37 °C under stirring in the dark. After 2 h, 20 mg of pancreatin and 125 mg of bile extract dissolved in 5 mL of 0.1 M NaHCO<sub>3</sub> were added, followed by a segment of cellulose dialysis tubing (molecular mass cutoff 12 kDa) containing 1.8 mL of 1 M NaHCO<sub>3</sub>. After 2 h of incubation at 37 °C, the solution that entered the dialysis tubing (taken as the IN sample) was separated, analyzed by HPLC and LC/MS and stored at −20 °C. In other experiments, BSP was exposed to the pH conditions of the general procedure, but without addition of the enzyme components and bile salts and the deriving IN sample was tested for its potential activity toward AD drug targets. When required, the IN sample was taken to pH 3 and extracted with ethyl acetate. Control experiments were run without addition of BSP.

### 3.5. AChE and BChE Inhibition Assays

The assays were performed as described [69] with slight modifications. Briefly, to 1.2 mL of 0.1 M phosphate buffer (pH 8.0) 40 µL of a solution of VA at different concentrations (0.006–6 mM) were added, followed by 40 µL of a 0.01 M ethanolic solution of DTNB and 40 µL of a 2.5 U/mL aqueous solution of the enzyme. After 5 min 8 µL of a 0.075 M aqueous solution of the substrate was added and after additional 2.5 min the absorbance at 412 nm was measured. For the reference value, 40 µL of water replaced the VA solution. For determining the blank value, 40 µL of water replaced the enzyme solution.

### 3.6. AChE-Induced A $\beta$ 1-40 Aggregation Inhibition Assay

The assay was performed as described [69] with slight modifications. The A $\beta$ 1-40 solution was prepared by suspending 1 mg of amyloid in 50  $\mu$ L of HFIP; the suspension was left to stay at room temperature for 4 h, after that the solvent was removed under a stream of argon. Briefly, to 0.15 mL of buffer solution (25 mM NaH<sub>2</sub>PO<sub>4</sub>, 100 mM NaCl, pH 8.0) 15  $\mu$ L of 100  $\mu$ M solution of VA or of IN sample, followed by 120  $\mu$ L of a 2.5 U/mL buffer solution of AChE and 15  $\mu$ L of a 2 mM DMSO solution of HFIP-pretreated A $\beta$ 1-40 were added. After 5 h 60  $\mu$ L of a 15  $\mu$ M buffer solution of thioflavin T were added and after additional 5 min the fluorescence emission at 482 nm ( $\lambda_{ex}$  = 450 nm) was measured. For the reference value, 15  $\mu$ L of water replaced the inhibitor solution. For determining the blank value, 15  $\mu$ L of DMSO replaced the A $\beta$  solution.

### 3.7. Self-Induced A $\beta$ 1-42 Aggregation Inhibition Assay

The assay was performed as described [75] with slight modifications. A 0.5 mM stock solution of A $\beta$ 1-42 was prepared in DMSO and diluted 1:10 in 0.05 M phosphate buffer solution containing 0.1 M NaCl (pH 7.5). To 30  $\mu$ L of the amyloid solution 30  $\mu$ L of 10–100  $\mu$ M solution of VA or of IN sample (undiluted or diluted 1:3 in water) were added. After 24 h incubation at 37 °C, 240  $\mu$ L of a 5  $\mu$ M thioflavin T in 50 mM glycine-NaOH buffer (pH 8.5) were added and after 5 min the fluorescence emission at 490 nm ( $\lambda_{ex}$  = 446 nm) was measured. For the reference value, 30  $\mu$ L of water replaced the inhibitor solution.

### 3.8. BACE-1 Inhibition Assay

The assay was carried out according to the supplied manual. Briefly, to 1.02 mL of buffer 150  $\mu$ L of 60–600  $\mu$ M VA solution or of IN sample (diluted 1:10 or 1:100 in water) were added, followed by 300  $\mu$ L of the substrate solution and 30  $\mu$ L of enzyme solution. After 2 h incubation at 37 °C, 600  $\mu$ L of the stop solution were added and the fluorescence emission at 405 nm ( $\lambda_{ex}$  = 320 nm) was measured. For the reference value, 150  $\mu$ L of water replaced the inhibitor solution. For determining the blank value, 30  $\mu$ L of buffer replaced the enzyme solution.

## 4. Conclusions

We have reported herein that black sesame pigment is transformed under the conditions of simulated gastrointestinal digestion, although the amount of the low molecular weight components released is relatively low (<10% on a *w/w* basis) compared to the pigment treated. Most of the transformations occurred under the pH conditions mimicking the intestinal environment, and were due to moderate alkaline hydrolytic reaction rather than the action of the enzymes.

All of the components released have a potential to pass into the serum as evidenced by the serum availability model used. One of the most abundant of these components proved to be vanillic acid, a result of considerable interest in light of the several beneficial properties of this compound.

More than 80% inhibition of the acetylcholinesterase-induced A $\beta$ 1-40 aggregation was observed in the presence of the potentially bioaccessible (soluble) fraction from the simulated digestion of the pigment, which also efficiently inhibited self-induced A $\beta$ 1-42 aggregation and  $\beta$ -secretase activity even after extensive dilution.

These properties open new perspectives toward the use of black sesame pigment, an easy to handle and stable material that could be obtained from a low cost source and purified through a scalable procedure, as a food supplement for the prevention of amyloid aggregation.

**Supplementary Materials:** Supplementary materials are available online: <http://www.mdpi.com/1420-3049/23/3/676/s1>. Figure S1: HPLC trace of a standard mixture containing 3,4-dihydroxybenzoic acid, 4-hydroxybenzoic acid and VA (same elution conditions of Figure 1), Figure S2: UV and mass spectra of the products A, B and C of Figure 1, Figure S3: MS spectrum of the product eluted at 12.5 min and HPLC trace of standard VA (under the same elution conditions of Figure 2), Figure S4: AChE inhibition by VA. Reported are the mean + SD values from



at least three experiments, Figure S5: BChE inhibition by VA. Reported are the mean + SD values from at least three experiments.

**Author Contributions:** Lucia Panzella, Thomas Eidenberger and Alessandra Napolitano conceived and designed the experiments; Lucia Panzella performed the experiments and analyzed the data; Lucia Panzella, Thomas Eidenberger and Alessandra Napolitano contributed to writing the paper.

**Conflicts of Interest:** The authors declare no conflict of interest.

## References

1. Palanimuthu, D.; Poon, R.; Sahni, S.; Anjum, R.; Hibbs, D.; Lin, H.Y.; Bernhardt, P.V.; Kalinowski, D.S.; Richardson, D.R. A novel class of thiosemicarbazones show multi-functional activity for the treatment of Alzheimer's disease. *Eur. J. Med. Chem.* **2017**, *139*, 612–632. [[CrossRef](#)] [[PubMed](#)]
2. Francis, P.T.; Palmer, A.M.; Snape, M.; Wilcock, G.K. The cholinergic hypothesis of Alzheimer's disease: A review of progress. *J. Neurol. Neurosurg. Psychiatry* **1999**, *66*, 137–147. [[CrossRef](#)] [[PubMed](#)]
3. Ayton, S.; Lei, P.; Bush, A.I. Metallostasis in Alzheimer's disease. *Free Radic. Biol. Med.* **2013**, *62*, 76–89. [[CrossRef](#)] [[PubMed](#)]
4. LaFerla, F.M.; Oddo, S. Alzheimer's disease: A $\beta$ , tau and synaptic dysfunction. *Trends Mol. Med.* **2005**, *11*, 170–176. [[CrossRef](#)] [[PubMed](#)]
5. Barnham, K.J.; Masters, C.L.; Bush, A.I. Neurodegenerative diseases and oxidative stress. *Nat. Rev. Drug Discov.* **2004**, *3*, 205–214. [[CrossRef](#)] [[PubMed](#)]
6. Viayna, E.; Sola, I.; Bartolini, M.; De Simone, A.; Tapia-Rojas, C.; Serrano, F.G.; Sabaté, R.; Juárez-Jiménez, J.; Pérez, B.; Luque, F.J.; et al. Synthesis and multitarget biological profiling of a novel family of rhein derivatives as disease-modifying anti-Alzheimer agents. *J. Med. Chem.* **2014**, *57*, 2549–2567. [[CrossRef](#)] [[PubMed](#)]
7. Penke, B.; Bogár, F.; Fülöp, L.  $\beta$ -Amyloid and the pathomechanisms of Alzheimer's disease: A comprehensive view. *Molecules* **2017**, *22*, 1692. [[CrossRef](#)] [[PubMed](#)]
8. Hardy, J.; Selkoe, D.J. The amyloid hypothesis of Alzheimer's disease: Progress and problems on the road to therapeutics. *Science* **2002**, *297*, 353–356. [[CrossRef](#)] [[PubMed](#)]
9. Kung, H.F. The  $\beta$ -amyloid hypothesis in Alzheimer's disease: Seeing is believing. *ACS Med. Chem. Lett.* **2012**, *3*, 265–267. [[CrossRef](#)] [[PubMed](#)]
10. Bezerra da Silva, C.; Pott, A.; Elifio-Esposito, S.; Dalarmi, L.; Fialho do Nascimento, K.; Moura Burci, L.; de Oliveira, M.; de Fátima Gaspari Dias, J.; Warumby Zanin, S.M.; Gomes Miguel, O.; et al. Effect of donepezil, tacrine, galantamine and rivastigmine on acetylcholinesterase inhibition in *Dugesia tigrina*. *Molecules* **2016**, *21*, 53. [[CrossRef](#)] [[PubMed](#)]
11. Lipton, S.A. The molecular basis of memantine action in Alzheimer's disease and other neurologic disorders: Low-affinity, uncompetitive antagonism. *Curr. Alzheimer Res.* **2005**, *2*, 155–165. [[CrossRef](#)] [[PubMed](#)]
12. Wang, Q.; Yu, X.; Li, L.; Zheng, J. Inhibition of amyloid- $\beta$  aggregation in Alzheimer's disease. *Curr. Pharm. Des.* **2014**, *20*, 1223–1243. [[CrossRef](#)] [[PubMed](#)]
13. Hiremathad, A.; Piemontese, L. Heterocyclic compounds as key structures for the interaction with old and new targets in Alzheimer's disease therapy. *Neural Regen. Res.* **2017**, *12*, 1256–1261. [[PubMed](#)]
14. Bachurin, S.O.; Bovina, E.V.; Ustyugov, A.A. Drugs in clinical trials for Alzheimer's disease: The major trends. *Med. Res. Rev.* **2017**, *37*, 1186–1225. [[CrossRef](#)] [[PubMed](#)]
15. Inestrosa, N.C.; Alvarez, A.; Pérez, C.A.; Moreno, R.D.; Vicente, M.; Linker, C.; Casanueva, O.I.; Soto, C.; Garridom, J. Acetylcholinesterase accelerates assembly of amyloid-beta-peptides into Alzheimer's fibrils: Possible role of the peripheral site of the enzyme. *Neuron* **1996**, *16*, 881–891. [[CrossRef](#)]
16. Johnson, G.; Moore, S.W. The peripheral anionic site of acetylcholinesterase: Structure, functions and potential role in rational drug design. *Curr. Pharm. Des.* **2006**, *12*, 217–225. [[CrossRef](#)] [[PubMed](#)]
17. Li, B.; Huang, A.-L.; Zhang, Y.-L.; Li, Z.; Ding, H.-W.; Huang, C.; Meng, X.-M.; Li, J. Design, synthesis and evaluation of hesperetin derivatives as potential multifunctional anti-Alzheimer agents. *Molecules* **2017**, *22*, 1067. [[CrossRef](#)] [[PubMed](#)]
18. Sang, Z.; Pan, W.; Wang, K.; Ma, Q.; Yu, L.; Liu, W. Design, synthesis and biological evaluation of 3,4-dihydro-2(1H)-quinoline-O-alkylamine derivatives as new multipotent cholinesterase/monoamine oxidase inhibitors for the treatment of Alzheimer's disease. *Bioorg. Med. Chem.* **2017**, *25*, 3006–3017. [[CrossRef](#)] [[PubMed](#)]

19. Jameel, E.; Meena, P.; Maqbool, M.; Kumar, J.; Ahmed, W.; Mumtazuddin, S.; Tiwari, M.; Hoda, N.; Jayaram, B. Rational design, synthesis and biological screening of triazine-triazolopyrimidine hybrids as multitarget anti-Alzheimer agents. *Eur. J. Med. Chem.* **2017**, *136*, 36–51. [[CrossRef](#)] [[PubMed](#)]
20. Sang, Z.; Qiang, X.; Li, Y.; Xu, R.; Cao, Z.; Song, Q.; Wang, T.; Zhang, X.; Liu, H.; Tan, Z.; et al. Design, synthesis and evaluation of scutellarein-O-acetamidoalkylbenzylamines as potential multifunctional agents for the treatment of Alzheimer's disease. *Eur. J. Med. Chem.* **2017**, *135*, 307–323. [[CrossRef](#)] [[PubMed](#)]
21. Maqbool, M.; Manral, A.; Jameel, E.; Kumar, J.; Saini, V.; Shandilya, A.; Tiwari, M.; Hoda, N.; Jayaram, B. Development of cyanopyridine-triazine hybrids as lead multitarget anti-Alzheimer agents. *Bioorg. Med. Chem.* **2016**, *24*, 2777–2788. [[CrossRef](#)] [[PubMed](#)]
22. Mazzanti, G.; Di Giacomo, S. Curcumin and resveratrol in the management of cognitive disorders: What is the clinical evidence? *Molecules* **2016**, *21*, 124. [[CrossRef](#)] [[PubMed](#)]
23. Spagnuolo, C.; Napolitano, M.; Tedesco, I.; Moccia, S.; Milito, A.; Russo, G.L. Neuroprotective role of natural polyphenols. *Curr. Top. Med. Chem.* **2016**, *16*, 1943–1950. [[CrossRef](#)] [[PubMed](#)]
24. Malar, D.S.; Devi, K.P. Dietary polyphenols for treatment of Alzheimer's disease—Future research and development. *Curr. Pharm. Biotechnol.* **2014**, *15*, 330–342. [[CrossRef](#)] [[PubMed](#)]
25. Ngoungoure, V.L.; Schluesener, J.; Moundipa, P.F.; Schluesener, H. Natural polyphenols binding to amyloid: A broad class of compounds to treat different human amyloid diseases. *Mol. Nutr. Food Res.* **2015**, *59*, 8–20. [[CrossRef](#)] [[PubMed](#)]
26. Stefani, M.; Rigacci, S. Beneficial properties of natural phenols: Highlight on protection against pathological conditions associated with amyloid aggregation. *Biofactors* **2014**, *40*, 482–493. [[CrossRef](#)] [[PubMed](#)]
27. Moncalvo, A.; Marinoni, L.; Dordoni, R.; Duserm Garrido, G.; Lavelli, V.; Spigno, G. Waste grape skins: Evaluation of safety aspects for the production of functional powders and extracts for the food sector. *Food Addit. Contam. Part A Chem. Anal. Control Expo. Risk Assess.* **2016**, *33*, 1116–1126. [[CrossRef](#)] [[PubMed](#)]
28. Piemontese, L. Plant food supplements with antioxidant properties for the treatment of chronic and neurodegenerative diseases: Benefits or risks? *J. Diet. Suppl.* **2017**, *14*, 478–484. [[CrossRef](#)] [[PubMed](#)]
29. Liu, Z.; Chen, Y.; Qiao, Q.; Sun, Y.; Liu, Q.; Ren, B.; Liu, X. Sesamol supplementation prevents systemic inflammation-induced memory impairment and amyloidogenesis via inhibition of nuclear factor kappaB. *Mol. Nutr. Food Res.* **2017**, *61*. [[CrossRef](#)]
30. Katayama, S.; Sugiyama, H.; Kushimoto, S.; Uchiyama, Y.; Hirano, M.; Nakamura, S. Effects of sesaminol feeding on brain A $\beta$  accumulation in a senescence-accelerated mouse-prone 8. *J. Agric. Food Chem.* **2016**, *64*, 4908–4913. [[CrossRef](#)] [[PubMed](#)]
31. Misra, S.; Tiwari, V.; Kuhad, A.; Chopra, K. Modulation of nitregeric pathway by sesamol prevents cognitive deficits and associated biochemical alterations in intracerebroventricular streptozotocin administered rats. *Eur. J. Pharmacol.* **2011**, *659*, 177–186. [[CrossRef](#)] [[PubMed](#)]
32. Um, M.Y.; Ahn, J.Y.; Kim, S.; Kim, M.K.; Ha, T.Y. Sesaminol glucosides protect  $\beta$ -amyloid peptide-induced cognitive deficits in mice. *Biol. Pharm. Bull.* **2009**, *32*, 1516–1520. [[CrossRef](#)] [[PubMed](#)]
33. Zhou, L.; Lin, X.; Abbasi, A.M.; Zheng, B. Phytochemical contents and antioxidant and antiproliferative activities of selected black and white sesame seeds. *Biomed. Res. Int.* **2016**, *2016*, 8495630. [[CrossRef](#)] [[PubMed](#)]
34. Kim, J.H.; Seo, W.D.; Lee, S.K.; Lee, Y.B.; Park, C.H.; Ryu, H.W.; Lee, J.H. Comparative assessment of compositional components, antioxidant effects, and lignan extractions from Korean white and black sesame (*Sesamum indicum* L.) seeds for different crop years. *J. Funct. Foods* **2014**, *7*, 495–505. [[CrossRef](#)]
35. Shahidi, F.; Liyana-Pathirana, C.M.; Wall, D.S. Antioxidant activity of white and black sesame seeds and their hull fractions. *Food Chem.* **2006**, *99*, 478–483. [[CrossRef](#)]
36. Namiki, M. The chemistry and physiological functions of sesame. *Food Rev. Int.* **1985**, *11*, 281–329. [[CrossRef](#)]
37. Kuo, P.C.; Lin, M.C.; Chen, G.F.; Yiu, T.J.; Tzen, J.T.C. Identification of methanol-soluble compounds in sesame and evaluation of antioxidant potential of its lignans. *J. Agric. Food Chem.* **2011**, *59*, 3214–3219. [[CrossRef](#)] [[PubMed](#)]
38. Reshma, M.V.; Balachandran, C.; Arumughan, C.; Sunderasan, A.; Divya Sukumaran, S.T.; Saritha, S.S. Extraction, separation and characterisation of sesame oil lignan for nutraceutical applications. *Food Chem.* **2010**, *120*, 1041–1046. [[CrossRef](#)]
39. Ryu, S.N.; Ho, C.T.; Osawa, T. High performance liquid chromatographic determination of antioxidant lignan glycosides in some varieties of sesame. *J. Food Lipids* **1998**, *5*, 17–28. [[CrossRef](#)]

40. Dar, A.A.; Arumugam, N. Lignans of sesame: Purification methods, biological activities and biosynthesis—A review. *Bioorg. Chem.* **2013**, *50*, 1–10. [[CrossRef](#)] [[PubMed](#)]
41. Hsu, D.-Z.; Chu, P.-Y.; Chandrasekaran, V.R.M.; Liu, M.-Y. Sesame lignan sesamol protects against aspirin-induced gastric mucosal damage in rats. *J. Funct. Foods* **2009**, *1*, 349–355. [[CrossRef](#)]
42. Ma, J.Q.; Ding, J.; Zhang, L.; Liu, C.M. Hepatoprotective properties of sesamin against CCl<sub>4</sub> induced oxidative stress-mediated apoptosis in mice via JNK pathway. *Food Chem. Toxicol.* **2014**, *64*, 41–48. [[CrossRef](#)] [[PubMed](#)]
43. Park, S.H.; Ryu, S.N.; Bu, Y.; Kim, H.; Simon, J.E.; Kim, K.S. Antioxidant components as potential neuroprotective agents in sesame (*Sesamum indicum* L.). *Food Rev. Int.* **2010**, *26*, 103–121. [[CrossRef](#)]
44. Saeed, M.; Khalid, H.; Sugimoto, Y.; Efferth, T. The lignan (-)-sesamin reveals cytotoxicity toward cancer cells: Pharmacogenomic determination of genes associated with sensitivity or resistance. *Phytomedicine* **2014**, *21*, 689–696. [[CrossRef](#)] [[PubMed](#)]
45. Panzella, L.; Napolitano, A. Natural phenol polymers: Recent advances in food and health applications. *Antioxidants* **2017**, *6*, 30. [[CrossRef](#)] [[PubMed](#)]
46. Panzella, L.; Eidenberger, T.; Napolitano, A.; d'Ischia, M. Black sesame pigment: DPPH assay-guided purification, antioxidant/antinitrosating properties and identification of a degradative structural marker. *J. Agric. Food Chem.* **2012**, *60*, 8895–8901. [[CrossRef](#)] [[PubMed](#)]
47. Manini, P.; Panzella, L.; Eidenberger, T.; Giarra, A.; Cerruti, P.; Trifuoggi, M.; Napolitano, A. Efficient binding of heavy metals by black sesame pigment: Toward innovative dietary strategies to prevent bioaccumulation. *J. Agric. Food Chem.* **2016**, *64*, 890–897. [[CrossRef](#)] [[PubMed](#)]
48. Woimant, F.; Trocello, J.M. Disorders of heavy metals. *Handb. Clin. Neurol.* **2014**, *120*, 851–864. [[PubMed](#)]
49. Caito, S.; Aschner, M. Neurotoxicity of metals. *Handb. Clin. Neurol.* **2015**, *131*, 169–189. [[PubMed](#)]
50. Karas, M.; Jakubczyk, A.; Szymanowska, U.; Zlotek, U.; Zielinska, E. Digestion and bioavailability of bioactive phytochemicals. *Int. J. Food Sci. Technol.* **2017**, *52*, 291–305. [[CrossRef](#)]
51. Martins, N.; Barros, L.; Ferreira, I.C.F.R. In vivo antioxidant activity of phenolic compounds: Facts and gaps. *Trends Food Sci. Technol.* **2016**, *48*, 1–12. [[CrossRef](#)]
52. Bohn, T.; McDougall, G.J.; Alegria, A.; Alminger, M.; Arrigoni, E.; Aura, A.-M.; Brito, C.; Cilla, A.; El, S.N.; Karakaya, S.; et al. Mind the gap—deficits in our knowledge of aspects impacting the bioavailability of phytochemicals and their metabolites—A position paper focusing on carotenoids and polyphenols. *Mol. Nutr. Food Res.* **2015**, *59*, 1307–1323. [[CrossRef](#)] [[PubMed](#)]
53. Alminger, M.; Aura, A.-M.; Bohn, T.; Dufour, C.; El, S.N.; Gomes, A.; Karakaya, S.; Martinez-Cuesta, M.C.; McDougall, G.J.; Requena, T.; et al. In vitro models for studying secondary plant metabolite digestion and bioaccessibility. *Compr. Rev. Food Sci. Food Saf.* **2014**, *13*, 413–436. [[CrossRef](#)]
54. Marze, S. Bioavailability of nutrients and micronutrients: Advances in modeling and in vitro approaches. *Annu. Rev. Food Sci. Technol.* **2017**, *8*, 35–55. [[CrossRef](#)] [[PubMed](#)]
55. Lee, S.-J.; Lee, S.Y.; Chung, M.-S.; Hur, S.J. Development of novel in vitro human digestion systems for screening the bioavailability and digestibility of foods. *J. Funct. Foods* **2016**, *22*, 113–121. [[CrossRef](#)]
56. Cilla, A.; González-Sarrías, A.; Tomás-Barberán, F.A.; Espín, J.C.; Barberá, R. Availability of polyphenols in fruit beverages subjected to in vitro gastrointestinal digestion and their effects on proliferation, cell-cycle and apoptosis in human colon cancer Caco-2 cells. *Food Chem.* **2009**, *114*, 813–820. [[CrossRef](#)]
57. Papillo, V.A.; Vitaglione, P.; Graziani, G.; Gökmen, V.; Fogliano, V. Release of antioxidant capacity from five plant foods during a multistep enzymatic digestion protocol. *J. Agric. Food Chem.* **2014**, *62*, 4119–4126. [[CrossRef](#)] [[PubMed](#)]
58. Gil-Izquierdo, A.; Zafrilla, P.; Tomas-Barberan, F.A. An in vitro method to simulate phenolic compound release from the food matrix in the gastrointestinal tract. *Eur. Food Res. Technol.* **2002**, *214*, 155–159. [[CrossRef](#)]
59. McDougall, G.J.; Dobson, P.; Smith, P.; Blake, A.; Stewart, D. Assessing potential bioavailability of raspberry anthocyanins using an in vitro digestion system. *J. Agric. Food Chem.* **2005**, *53*, 5896–5904. [[CrossRef](#)] [[PubMed](#)]
60. Shao, Y.; Hu, Z.; Yu, Y.; Mou, R.; Zhu, Z.; Beta, T. Phenolic acids, anthocyanins, proanthocyanidins, antioxidant activity, minerals and their correlations in non-pigmented, red, and black rice. *Food Chem.* **2018**, *239*, 733–741. [[CrossRef](#)] [[PubMed](#)]

61. Tai, A.; Sawano, T.; Ito, H. Antioxidative properties of vanillic acid esters in multiple antioxidant assays. *Biosci. Biotechnol. Biochem.* **2012**, *76*, 314–318. [[CrossRef](#)] [[PubMed](#)]
62. Świsłocka, R.; Piekut, J.; Lewandowski, W. The relationship between molecular structure and biological activity of alkali metal salts of vanillic acid: Spectroscopic, theoretical and microbiological studies. *Spectrochim. Acta A Mol. Biomol. Spectrosc.* **2013**, *100*, 31–40. [[CrossRef](#)] [[PubMed](#)]
63. Prince, P.S.M.; Dhanasekar, K.; Rajakumar, S. Preventive effects of vanillic acid on lipids, bax, bcl-2 and myocardial infarct size on isoproterenol-induced myocardial infarcted rats: A biochemical and in vitro study. *Cardiovasc. Toxicol.* **2011**, *11*, 58–66. [[CrossRef](#)] [[PubMed](#)]
64. Kim, S.J.; Kim, M.C.; Um, J.Y.; Hong, S.H. The beneficial effect of vanillic acid on ulcerative colitis. *Molecules* **2010**, *15*, 7208–7217. [[CrossRef](#)] [[PubMed](#)]
65. Ul Amin, F.; Ali Shah, S.; Kim, M.O. Vanillic acid attenuates A $\beta$ 1–42-induced oxidative stress and cognitive impairment in mice. *Sci. Rep.* **2017**, *7*, 40753. [[CrossRef](#)] [[PubMed](#)]
66. Singh, J.C.; Kakalij, R.M.; Kshirsagar, R.P.; Kumar, B.H.; Komakula, S.S.; Diwan, P.V. Cognitive effects of vanillic acid against streptozotocin-induced neurodegeneration in mice. *Pharm. Biol.* **2015**, *53*, 630–636. [[CrossRef](#)] [[PubMed](#)]
67. Grossberg, G.T. Cholinesterase inhibitors for the treatment of Alzheimer’s disease: Getting on and staying on. *Curr. Ther. Res. Clin. Exp.* **2003**, *64*, 216–235. [[CrossRef](#)]
68. Kwong, H.C.; Mah, S.H.; Chia, T.S.; Quah, C.K.; Lim, G.K.; Kumar, C.S.C. Cholinesterase inhibitory activities of adamantyl-based derivatives and their molecular docking studies. *Molecules* **2017**, *22*, 1005. [[CrossRef](#)] [[PubMed](#)]
69. Chen, X.; Wehle, S.; Kuzmanovic, N.; Merget, B.; Holzgrabe, U.; König, B.; Sotriffer, C.A.; Decker, M. Acetylcholinesterase inhibitors with photoswitchable inhibition of  $\beta$ -amyloid aggregation. *ACS Chem. Neurosci.* **2014**, *5*, 377–389. [[CrossRef](#)] [[PubMed](#)]
70. Acheson, S.A.; Quinn, D.M. Anatomy of acetylcholinesterase catalysis: Reaction dynamics analogy for human erythrocyte and electric eel enzymes. *Biochim. Biophys. Acta* **1990**, *1040*, 199–205. [[CrossRef](#)]
71. Greig, N.H.; Utsuki, T.; Yu, Q.; Zhu, X.; Holloway, H.W.; Perry, T.; Lee, B.; Ingram, D.K.; Lahiri, D.K. A new therapeutic target in Alzheimer’s disease treatment: Attention to butyrylcholinesterase. *Curr. Med. Res. Opin.* **2001**, *17*, 159–165. [[CrossRef](#)] [[PubMed](#)]
72. Li, Q.; Yang, H.; Chen, Y.; Sun, H. Recent progress in the identification of selective butyrylcholinesterase inhibitors for Alzheimer’s disease. *Eur. J. Med. Chem.* **2017**, *132*, 294–309. [[CrossRef](#)] [[PubMed](#)]
73. Mori, H.; Takio, K.; Ogawara, M.; Selkoe, D.J. Mass spectrometry of purified amyloid beta protein in Alzheimer’s disease. *J. Biol. Chem.* **1992**, *267*, 17082–17086. [[PubMed](#)]
74. Schmidt, M.; Sachse, C.; Richter, W.; Xu, C.; Fändrich, M.; Grigorieff, N. Comparison of Alzheimer A $\beta$ (1–40) and A $\beta$ (1–42) amyloid fibrils reveals similar protofilament structures. *Proc. Natl. Acad. Sci. USA* **2009**, *106*, 19813–19818. [[CrossRef](#)] [[PubMed](#)]
75. Qiang, X.; Sang, Z.; Yuan, W.; Li, Y.; Liu, Q.; Bai, P.; Shi, Y.; Ang, W.; Tan, Z.; Deng, Y. Design, synthesis and evaluation of genistein-O-alkylbenzylamines as potential multifunctional agents for the treatment of Alzheimer’s disease. *Eur. J. Med. Chem.* **2014**, *76*, 314–331. [[CrossRef](#)] [[PubMed](#)]
76. Näslund, J.; Schierhorn, A.; Hellman, U.; Lannfelt, L.; Roses, A.D.; Tjernberg, L.O.; Silberring, J.; Gandy, S.E.; Winblad, B.; Greengard, P.; et al. Relative abundance of Alzheimer A beta amyloid peptide variants in Alzheimer disease and normal aging. *Proc. Natl. Acad. Sci. USA* **1994**, *91*, 8378–8382. [[CrossRef](#)] [[PubMed](#)]
77. Hiremathad, A.; Keri, R.S.; Esteves, A.R.; Cardoso, S.M.; Chaves, S.; Santos, M.A. Novel tacrine-hydroxyphenylbenzimidazole hybrids as potential multitarget drug candidates for Alzheimer’s disease. *Eur. J. Med. Chem.* **2018**, *148*, 255–267. [[CrossRef](#)] [[PubMed](#)]
78. Briante, R.; Febbraio, F.; Nucci, R. Antioxidant properties of low molecular weight phenols present in the mediterranean diet. *J. Agric. Food Chem.* **2003**, *51*, 6975–6981. [[CrossRef](#)] [[PubMed](#)]
79. Rampa, A.; Tarozzi, A.; Mancini, F.; Pruccoli, L.; Di Martino, R.M.; Gobbi, S.; Bisi, A.; De Simone, A.; Palomba, F.; Zaccheroni, N.; et al. Naturally inspired molecules as multifunctional agents for Alzheimer’s disease treatment. *Molecules* **2016**, *21*, 643. [[CrossRef](#)] [[PubMed](#)]
80. Ghosh, A.K.; Brindisi, M.; Tang, J. Developing  $\beta$ -secretase inhibitors for treatment of Alzheimer’s disease. *J. Neurochem.* **2012**, *120*, 71–83. [[CrossRef](#)] [[PubMed](#)]

81. Kang, J.E.; Cho, J.K.; Curtis-Long, M.J.; Ryu, H.W.; Kim, J.H.; Kim, H.J.; Yuk, H.J.; Kim, D.W.; Park, K.H. Inhibitory evaluation of sulfonamide chalcones on  $\beta$ -secretase and acylcholinesterase. *Molecules* **2013**, *18*, 140–153. [[CrossRef](#)] [[PubMed](#)]
82. Jung, H.A.; Lee, E.J.; Kim, J.S.; Kang, S.S.; Lee, J.H.; Min, B.S.; Choi, J.S. Cholinesterase and BACE1 inhibitory diterpenoids from *Aralia cordata*. *Arch. Pharm. Res.* **2009**, *32*, 1399–1408. [[CrossRef](#)] [[PubMed](#)]
83. Fernández-Bachiller, M.I.; Pérez, C.; Monjas, L.; Rademann, J.; Rodríguez-Franco, M.I. New tacrine-4-oxo-4H-chromene hybrids as multifunctional agents for the treatment of Alzheimer's disease, with cholinergic, antioxidant, and  $\beta$ -amyloid-reducing properties. *J. Med. Chem.* **2012**, *55*, 1303–1317. [[CrossRef](#)] [[PubMed](#)]

**Sample Availability:** The IN sample is available from the authors.



© 2018 by the authors. Licensee MDPI, Basel, Switzerland. This article is an open access article distributed under the terms and conditions of the Creative Commons Attribution (CC BY) license (<http://creativecommons.org/licenses/by/4.0/>).